RAPID COMMUNICATIONS IN MASS SPECTROMETRY
Rapid Commun. Mass Spectrom. 2006; **20**: 3483–3487
Published online in Wiley InterScience (www.interscience.wiley.com) DOI: 10.1002/rcm.2744

RCM

Letter to the Editor

To the Editor-in-Chief
Sir,

Analysis of rosuvatatin by imaging mass spectrometry

Imaging matrix-assisted laser desorption/ionization (IM-MALDI)[1–5] and laser desorption ionization (IM-LDI)[6] have been used for the direct analysis of molecular distribution. IM-MALDI has been successfully used for the analysis of both high molecular weight (e.g. proteins),[1] medium molecular weight (e.g. peptides),[2] and low molecular weight (e.g. drugs, pharmaceutical compounds)[3,4,7] molecules in tissue sections. For measurements of biomacromolecules, the mass spectrometer is usually a time-of-flight (TOF) analyzer[8] operated in linear MS mode because this analyzer provides high scan speed, good mass resolution and high mass accuracy. Although other mass analyzers, such as ion traps, have recently been used to obtain surface analyte distribution by means of desorption electrospray (DESI),[9] the TOF remains the most widely used analyzer for this application. Its high scan speed makes it well suited for use with a MALDI source operating at high laser frequency (typically 200 Hz) thus minimizing the time needed to acquire the image.[10]

Multiple ion images can be constructed from a single tissue section. For the analysis of low molecular weight compounds, several workers have described sample preparation, and MALDI optimization, using the reflectron mode to increase resolution and mass accuracy.[3,4,7,11,12] To increase the selectivity and sensitivity of IM-MALDI techniques, images can be obtained by fragmenting the analyte $[M+H]^+$ ion and then monitoring specific product ions. Isolation, analyte fragmentation and product ion m/z values are usually obtained by using a quadrupole collision-induced dissociation time-of-flight analyzer (QqTOF)[3,11] or time-of-flight/time-of-flight (TOF/TOF)[4] instruments.

Another approach used to obtain analyte fragmentation is in-source decay.[13] In this case the laser energy is increased to observe in-source degradation of an analyte ion. The image is obtained by monitoring m/z values of both the precursor ion and selected product ions. Some studies have been performed using multivariate statistical image analysis (like principal component analysis) that can group spectral features (such as precursor and product ions appearing in the same location).[14,15] Thanks to these approaches it has been possible to identify regions of the sample surface that show common spectral features so as to localize the positions of the target compounds.

In this study IM-MALDI and IM-LDI experimental conditions were optimized to analyze rosuvastatin (a statin family compound), an important 3-hydroxy-3-methylglutaryl coenzyme A reductase inhibitor approved for the treatment of dislipidemia A.[16–18] The images were obtained by monitoring both the $[M+H]^+$ precursor ion and product ions obtained by in-source fragmentation. The data obtained by averaging the $[M+H]^+$ precursor ion and the in-source product ion images are reported and discussed. It should be emphasized that no mass spectrometric imaging method has, to date, been reported for the analysis of this drug in tissue samples.

Acetonitrile, trifluoroacetic acid (TFA), alpha-hydroxycinnamic acid (CHCA), sinapinic acid (SA), and dihydroxybenzoic acid (DHB) and calibrating molecules (bradykinin fragment 1–7, insulin oxidized B chain, angiotensin II, ACTH fragment 18–39) were purchased from Sigma Aldrich (Milan, Italy). Rosuvastatin (Scheme 1) was kindly provided by AstraZeneca (Macclesfield, UK). The mass spectrometer was calibrated by external calibration before each image acquisition.

Rat brain tissue samples were excised using a Microm (Walldorf, Germany) HM505E micrometer. The tissue was cut maintaining a brain temperature of −20°C to give a brain tissue depth of 14 micrometers. The rat brain tissue section was attached to the MALDI probe steel surface, maintaining a temperature of −20°C. The rosuvastatin and matrix were added to the MALDI steel plate and to the rat brain tissue section by hand spot deposition (500 nL/spot). The amount of rosuvastatin per spot was in the range 0.1–10 ng. The matrix concentration was 10 mg/mL for each matrix tested.

Spectra were acquired by means of a Voyager-DE STR MALDI (Applied Biosystems, Foster City, CA, USA) TOF mass spectrometer capable of operating in linear or reflectron mode and in delayed extraction conditions. The spectra were acquired in reflectron mode and the extraction delay time was 100 ns. A nitrogen laser operating at a laser wavelength of 337 nm was used. The nitrogen laser operates at 20 Hz with adjustable laser energy. The in-source dissociation of the rosuvastatin $[M+H]^+$ ion was optimized by adjusting the laser energy between 40 and 110 μJ. The accelerating voltage was 25 kV and the grid voltage was 75% of the accelerating voltage. The software option named 'idle power off time' was turned off during image acquisition to avoid automatic locking of the target plate potential after a defined time. The spectra were acquired in the m/z 200–500 range. The mass resolution in the acquisition m/z range was 20 000 and the mass accuracy was between 20 and 50 ppm.

The sample stage was moved automatically from one spot to another during the image acquisition process. Ten spectra were averaged for each image pixel. The spatial resolution was 100 and 250 μm, respectively, moving on the y and x axes. Ion density images were obtained by plotting the spatial dimensions of y and x vs. the signal amplitude of the selected ion range.

Images were obtained using MMSIT tool software.[19] The Applied Biosystems

RCM

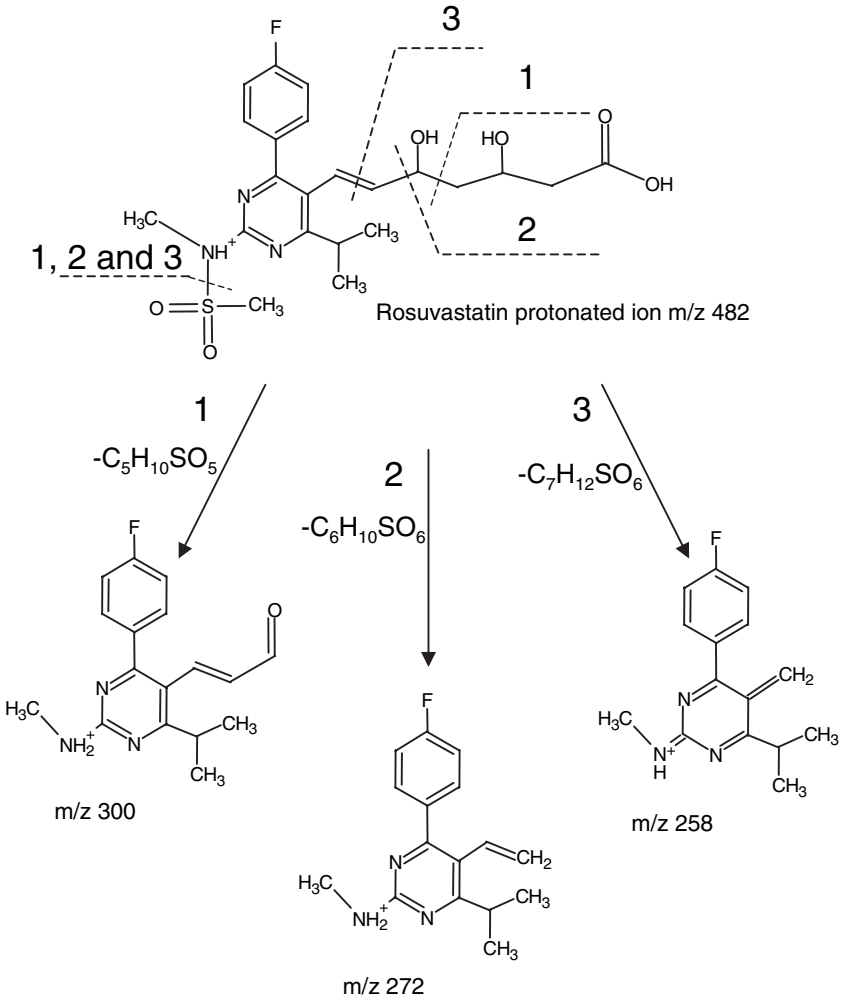

Scheme 1.

Voyager version 5 acquisition software was used to acquire in-source decay LDI and MALDI spectra using different laser energies and to obtain the x and y coordinates to be inserted in the MMSIT software to acquire the images. Data explorer software was used to elaborate the in-source decay spectra to study the rosuvastatin fragmentation pathway. The software SPIDER (freely available on the internet[20]) was used to obtain the average images. The images were exported in ASCII format and converted to SPIDER format using a home-made perl script.

A preliminary investigation was performed on rosuvastatin pure standard compounds on a MALDI steel plate to evaluate the best matrix to be used for the analysis. The analyses were initially performed by depositing 10 ng of rosuvastatin on the MALDI plate. Three matrices were tested (CHCA, SA and DHB) and the $[M+H]^+$ ion at *m/z* 482 for rosuvastatin was detected using all matrices (data not shown). The signal-to-noise (S/N) ratios achieved show that CHCA offers the best result (CHCA S/N: 501, SA S/N: 203 and DHB S/N: 305). Emphasis must be given to the rosuvastatin UV spectrum (Fig. 1(a)) that shows a weak absorbance (absorbance 0.04, concentration 1×10^{-6} M) at 337 nm (frequency of MALDI employed). Thus, some experiments were also performed by LDI-MS in order to evaluate the performance of LDI in terms of sensitivity. The spectra obtained by analyzing 10 ng of rosuvastatin on a MALDI stainless steel plate using both MALDI (CHCA matrix, laser energy 55 μJ) and LDI (laser energy 75 μJ) are, respectively, reported in Figs. 1(b) and 1(c). As can be observed, only $[M+H]^+$ ions are detectable by MALDI, whereas $[M+H]^+$ and in-source product ions were obtained by LDI. These product ions could, hypothetically, originate from either photon-induced fragmentation directly occurring on the neutral molecules,[21] collisionally induced decomposition processes originating from $[M+H]^+$ species,[22] or thermal decomposition.[23] The fragmentation pathway leading to the most selective and abundant rosuvastatin product ions is shown in Scheme 1. These product ions could be formed in a single step from the $[M+H]^+$ ion by loss of $C_5H_{10}SO_5$ (leading to the ion at *m/z* 300), $C_6H_{10}SO_6$ (leading to *m/z* 272), and $C_7H_{12}SO_6$ (leading to *m/z* 258) with proton rearrangement. These ions have been selected on two bases: (a) the good mass accuracy (20–50 ppm) and (b) the fact that they have been observed previously in the LC/MS/MS fragmentation of rosuvastatin using a triple quadrupole mass analyzer.[24,25]

Different laser energy values were tested in order to obtain the best ionization conditions. The breakdown curves obtained by monitoring the $[M+H]^+$ precursor ion (*m/z* 482) and the most abundant product ion at *m/z* 300 vs. the laser energy using both MALDI and LDI are, respectively, shown in Figs. 2a-(i) and 2a-(ii). The breakdown curves obtained by monitoring the $[M+H]^+$ ion at *m/z* 482 and the in-source product ions at *m/z* 272 and 258 exhibit a similar trend (data not shown). In the case of MALDI, the $[M+H]^+$ ion is observed, without analyte fragmentation, by using a laser energy of 53 μJ (Fig. 2a-(i)) and the fragmentation process takes place from a laser energy of 61 μJ. By contrast, in the case of LDI, the $[M+H]^+$ ion and the product ions are observed starting from a laser energy of 73 μJ (Fig. 2a-(ii)) and no signal was detected using a lower laser energy. Moreover, several neutral losses, including loss of hydrogen, were observed with LDI but not with MALDI.

The presence of a strong background noise observed using LDI should be noted. In addition, if a low amount of rosuvastatin (0.1 ng) is deposited on the plate and irradiated by LDI (laser energy 73 μJ) low product ion formation can be observed, suggesting that a possible

DOI: 10.1002/rcm

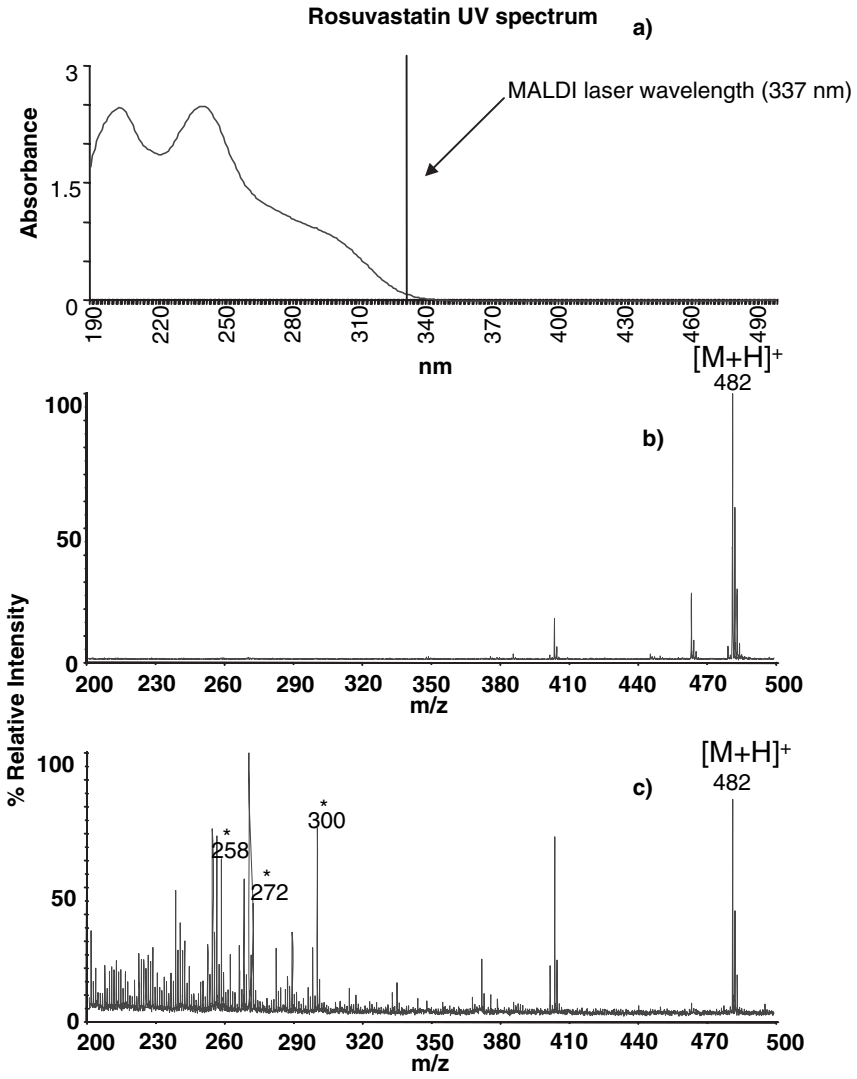

Figure 1. (a) UV spectrum of 1×10^{-6} M rosuvastatin solution, (b) MALDI spectrum (laser energy 55 μJ) obtained using CHCA as matrix (matrix concentration 10 ng/mL) on a steel plate, and (c) LDI spectrum (laser energy 75 μJ) analyzing 10 ng of rosuvastatin on a steel plate. *Rosuvastatin-specific in-source product ions.

fragmentation mechanism is analyte-analyte gas-phase collision after the ablation.[22] Indeed, when a low amount of analyte is deposited the analyte molecule surface density decreases as well as the number of ion-molecule collisions after the ablation. In fact, when MALDI is used the relative abundance of the product ions does not decrease. This is probably due to the high amount of matrix molecules that are obtained after the laser irradiation, independent of the analyte concentration. Thus, It is reasonable to assume that ion-molecule collisions take place between the analyte and the matrix leading to the analyte fragmentation reactions.

Based on the preliminary investigation described above, the MALDI technique was chosen to perform the imaging study of rosuvastatin due to its stability and high S/N ratio. The images of the $[M+H]^+$ ion and the most abundant and selective product ions (*m/z* 300, 272 and 258) were obtained and averaged. As shown in Fig. 2a-(i) the stable laser energy region, in which both $[M+H]^+$ (most abundant ion) and product ions were observed, is between 61 and 72 μJ (lower dR/dw value; R is relative abundance and w is laser energy). In this region the product ion intensity is lower that that of the $[M+H]^+$ ion and the spectra are reproducible in terms of relative abundance. Thus, a laser energy of 68 μJ was used to acquire the images.

The image is shown in Fig. 2a-(iii)). An amount of 0.1 ng of rosuvastatin was deposited on the steel plate and CHCA was used as matrix. As can be observed the average image clearly shows the rosuvastatin distribution. The image of a matrix control spot, without the analyte, was acquired in order to show the selectivity of the selected ions (Fig. 2a-(iv)). As can be seen no image was obtained in this case.

These results led us to test this image approach on a complex biological matrix. A rat brain section, derived from a rat not treated with rosuvastatin, with a depth of 14 μm was placed on the MALDI sample plate and the matrix plus analyte was deposited in different regions (8 spots) of the brain surface to verify whether the ionization and fragmentation conditions changed when rosuvastatin was deposited on a complex matrix. Even in this case the best results in terms of S/N ratio were achieved using CHCA as matrix (CHCA S/N: 585, SA S/N: 250 and DHB S/N: 351; rosuvastatin spot amount 10 ng). The amount of rosuvastatin per spot ranges from 0.1 to 10 ng and breakdown curves were acquired in order to obtain the best conditions for the $[M+H]^+$ ion and the in-source product ions. Figure 2b-(i) shows the breakdown curves obtained by monitoring the $[M+H]^+$ ion at *m/z* 482 and the product ion at *m/z* 300 vs. the laser energy. The breakdown curves obtained in this case by monitoring the $[M+H]^+$ ion at *m/z* 482 vs. the in-source product ions at *m/z* 272 and 258 exhibit a similar trend (data not shown). The best performance in terms of stability of $[M+H]^+$ and product ion intensity (lower dR/dw value) was achieved in the laser energy range 73–78 μJ instead of the laser energy range 61–72 μJ obtained on the steel plate. This behavior can be rationalized by considering the matrix ionization suppression effect due to the wide number of biological compounds and inorganic salts present in rat brain. These compounds can give rise to the formation of adduct with the analyte (e.g. sodium and potassium adducts) preventing formation of the $[M+H]^+$ ion and the formation of related product ions. Thus, higher laser energy leads to an increase in energetic gas-phase matrix ions that compete with other salts and biological molecules in the analyte ionization. An average

DOI: 10.1002/rcm

RCM

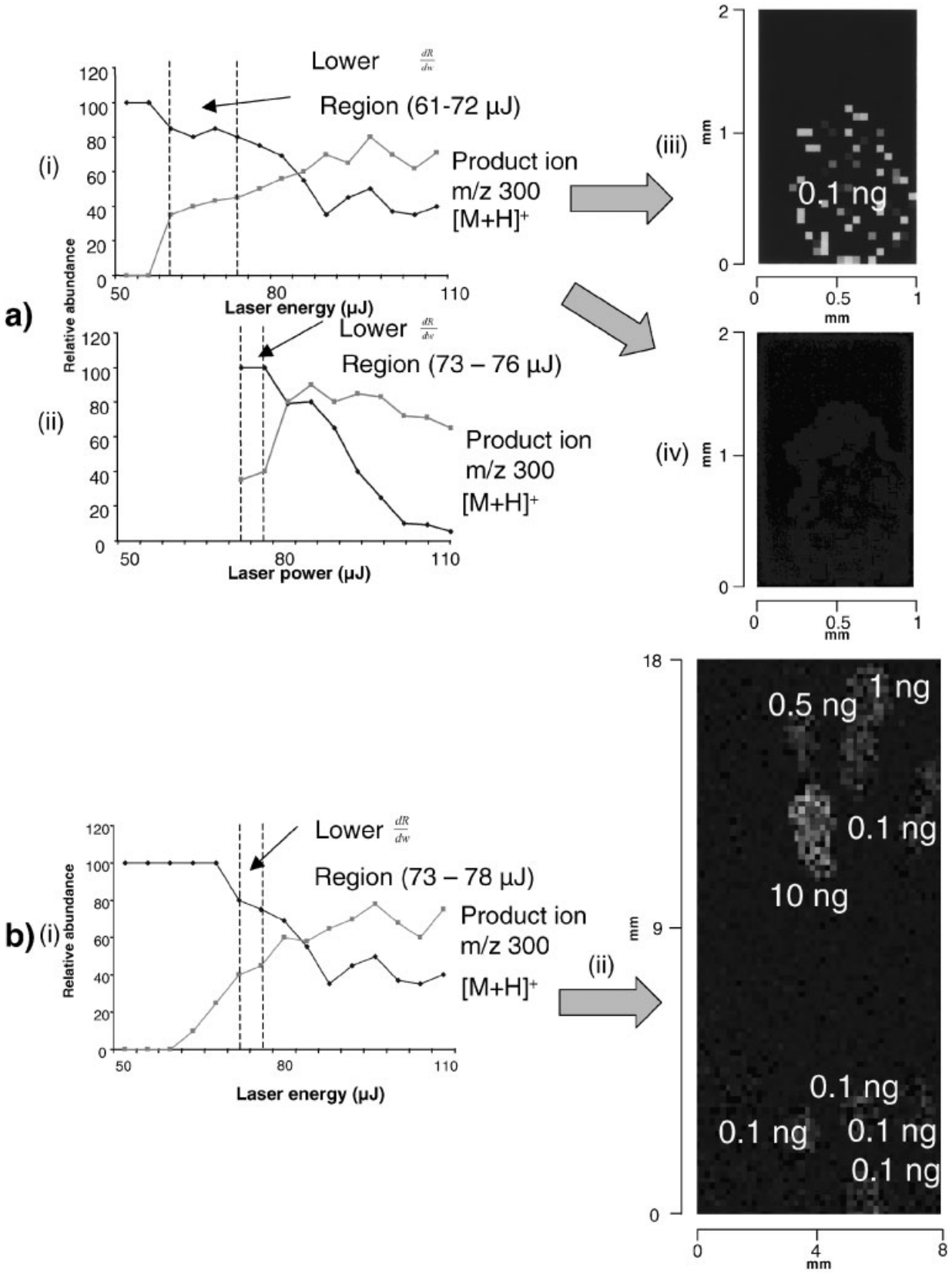

Figure 2. (a) Breakdown curves obtained by monitoring the rosuvastatin precursor ion at *m/z* 482 and the product ion at *m/z* 300 vs. laser energy. The breakdown curves were obtained using (i) MALDI and (ii) LDI. (iii) Average IM-MALDI image obtained using 68 µJ laser energy. (iv) Matrix only control spot image. (b) (i) MALDI breakdown curve obtained by monitoring the precursor and product ions (*m/z* 482 and 300, respectively, vs. laser energy) of the rosuvastatin deposited on rat brain tissue section (tissue depth 14 µm; rosuvastatin concentration 10 ng). (ii) Average IM-MALDI image obtained analyzing different analyte amounts (0.1–10 ng) on rat brain tissue section using a laser energy of 74 µJ. The rosuvastatin concentration for each spot is reported.

DOI: 10.1002/rcm

image from tissue was acquired using the image averaging approach with a laser energy of 74 μJ (Fig. 2b-(ii)). In the top section of the image different spots of rosuvastatin, ranging from 0.1 to 10 ng, were deposited providing defined images. Image reproducibility was also tested by depositing four spots containing 0.1 ng of rosuvastatin (bottom image section). In conclusion, well-defined reproducible images were achieved for rosuvastatin by IM-MALDI in conjunction with the image average elaboration approach.

Further studies are in progress in order to apply this method in the analysis of rosuvastatin in tissue samples of animals treated with this compound.

Simone Cristoni[1,2,3] Maura Brioschi[3,4], Andrea Rizzi[3], Luigi Sironi[4], Paolo Gelosa[4], Elena Tremoli[3,4], Luigi Rossi Bernardi[2] and Cristina Banfi[3,4]*
[1]Ion Source & Biotechnology, Milan, Italy
[2]University of Milan, CISI, Segrate, Milan, Italy
[3]Monzino Cardiological Center, IRCCS, Milan, Italy
[4]Department of Pharmacological Science, University of Milan, Milan, Italy

**Correspondence to: S. Cristoni, Monzino Cardiological Center, Via Parea 4, 20100 Milan, Italy.*
E-mail: simone.cristoni@virgilio.it

REFERENCES

1. Chaurand P, Schwartz SA, Reyzer ML, Caprioli RM. *Toxicol. Pathol.* 2005; **33**: 92.
2. Caprioli RM, Farmer TB, Gile J. *Anal. Chem.* 1997; **69**: 4751.
3. Crossman L, McHugh NA, Hsieh Y, Korfmacher WA, Chen J. *Rapid Commun. Mass Spectrom.* 2006; **20**: 284.
4. Wang HY, Jackson SN, McEuen J. *Anal. Chem.* 2005; **77**: 6682.
5. Stoeckli M, Farmer TB, Caprioli RM. *J. Am. Soc. Mass Spectrom.* 1999; **10**: 67.
6. Spengler B, Hubert M. *J. Am. Soc. Mass Spectrom.* 2002; **13**: 735.
7. Bunch J, Clench MR, Richards DS. *Rapid Commun. Mass Spectrom.* 2004; **18**: 3051.
8. Roepstorff P. *EXS* 2000; **88**: 81.
9. Van Berkel GJ, Kertesz V. *Anal. Chem.* 2006; **78**: 4938.
10. Moskovets E, Preisler J, Chen HS, Rejtar T, Andreev V, Karger BL. *Anal. Chem.* 2006; **78**: 912.
11. Reyzer ML, Hsieh Y, Ng K, Korfmacher WA, Caprioli RM. *J. Mass Spectrom.* 2003; **38**: 1081.
12. McCombie G, Knochenmuss R. *Anal. Chem.* 2004; **76**: 4990.
13. Gao J, Tsugita A, Takayama M, Xu L. *Anal. Chem.* 2002; **74**: 1449.
14. Sjovall P, Lausmaa J, Johansson B. *Anal. Chem.* 2004; **76**: 4271.
15. Ostrowski SG, Van Bell CT, Winograd N, Ewing AG. *Science* 2004; **305**: 71.
16. van Mil AH, Westendorp RG, Bollen EL, Lagaay AM, Blauw GJ. *Drugs* 2000; **59**: 1.
17. Sironi L, Gianazza E, Gelosa P, Guerrini U, Nobili E, Gianella A, Cremonesi B, Paoletti R, Tremoli E. *Arterioscler. Thromb. Vasc. Biol.* 2005; **25**: 598.
18. Lopez LM. *J. Am. Pharm. Assoc.* 2005; **45**: 503.
19. Available http://www.maldi-msi.org/.
20. Available http://www.wadsworth.org/spider_doc/spider/docs/master.html.
21. Sharma P, Vatsa RK, Maity DK, Kulshreshtha SK. *Rapid Commun. Mass Spectrom.* 2004; **18**: 2383.
22. Yamagaki T, Suzuki H, Tachibana K. *J. Am. Soc. Mass Spectrom.* 2006; **17**: 67.
23. Lin Q, Knochenmuss R. *Rapid Commun. Mass Spectrom.* 2001; **15**: 1422.
24. Xu DG, Ruan ZR, Zhou Q, Yuan H, Jiang B. *Rapid Commun. Mass Spectrom.* 2006; **20**: 2369.
25. Hull CK, Penman AD, Smith CK, Martin PD. *J. Chromatogr. B Analyt. Technol. Biomed. Life Sci.* 2002; **772**: 219.

Received 8 July 2006
Revised 9 September 2006
Accepted 14 September 2006

DOI: 10.1002/rcm